ADVANCED FUNCTIONAL MATERIALS

Supporting Information

for *Adv. Funct. Mater.*, DOI: 10.1002/adfm.201202466

Reactive Aramid Nanostructures as High-Performance Polymeric Building Blocks for Advanced Composites

*Keqin Cao, Carlos Pons Siepermann, Ming Yang, Anthony M. Waas, Nicholas A. Kotov, M. D. Thouless, and Ellen M. Arruda**

Submitted to ADVANCED FUNCTIONAL MATERIALS
DOI: 10.1002/adfm.201202466

Supporting Information

S1. SEM Images of Aramid Nanostructured Networks

Scanning Electron Microscopy was used to observe the surface and cross-sectional features of the aramid nanostructured networks. **Figure S1** (a-c) show the surface of a filtered film with no treatment at different magnifications. As shown in Figure S1.a, the surface was generally smooth except that at the edge. The roughness was probably caused by the proximity to the filtration funnel during the consolidation process. Figure S1 (b and c) reveal a dense structure at larger magnifications. Figure S1.d shows the cross-section of the film, which was a layered structure formed by the filtration method. Similar surface and cross-sectional features were observed in SEM of the filtered films with or without PA/GA treatment, as that level of detail cannot be resolved by SEM.

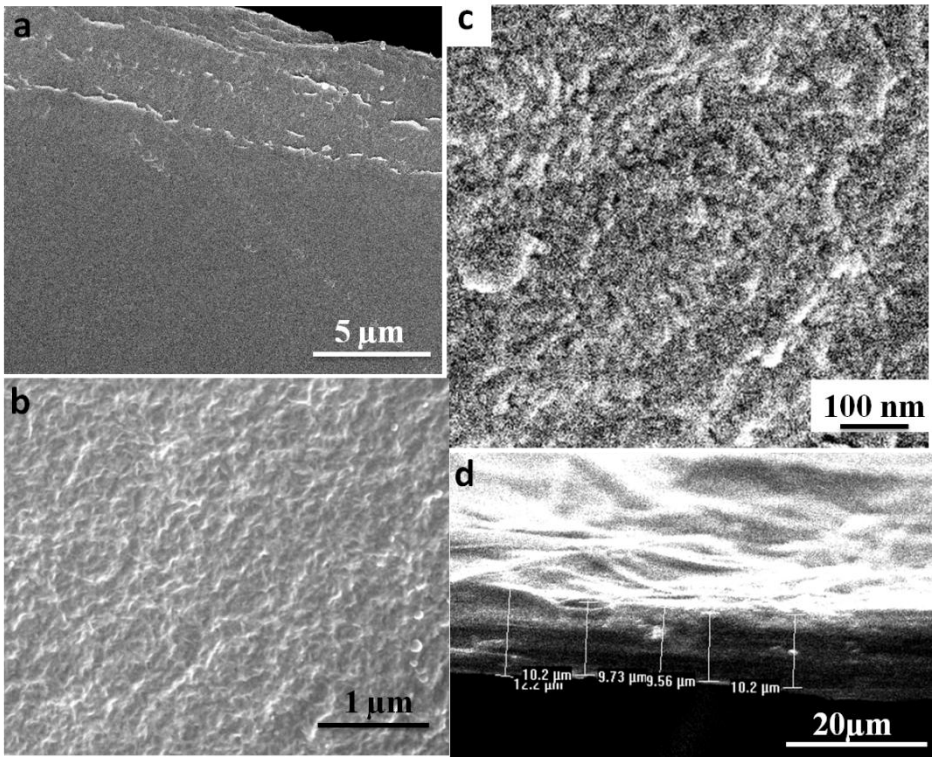

Figure S1. Scanning Electron Microscopy images of the filtered film with no treatment. The surface of the "No Treatment" film at different magnifications from small to large: a) a smooth surface away from the edge; b) and c) a densely bonded structure. d) The cross-section of the film. A layered structure was revealed. Similar surface and cross-sectional features of the PA/GA treated films were observed at these larger scales compared to TEM.

S2. Uniaxial Tensile Testing of Plain Woven Kevlar Mat

A commercial 0°/90° plain woven Kevlar mat was characterized by uniaxial tensile testing at 0.005 s^{-1}. The stress-strain curves are shown in **Figure S2**.a. The tests were conducted along the 0° fiber orientation, which is the strongest axis of the Kevlar mat. The fibers in the 90° direction were free to slide during the tests, (Figure S2.b). This freedom to slide during deformation possibly yielded a higher strain-energy density. Figure S2 (c and d) show the comparison between the mat before and after testing. Single fiber breakages (Figure S2.d) caused the gradual failure of the mat.

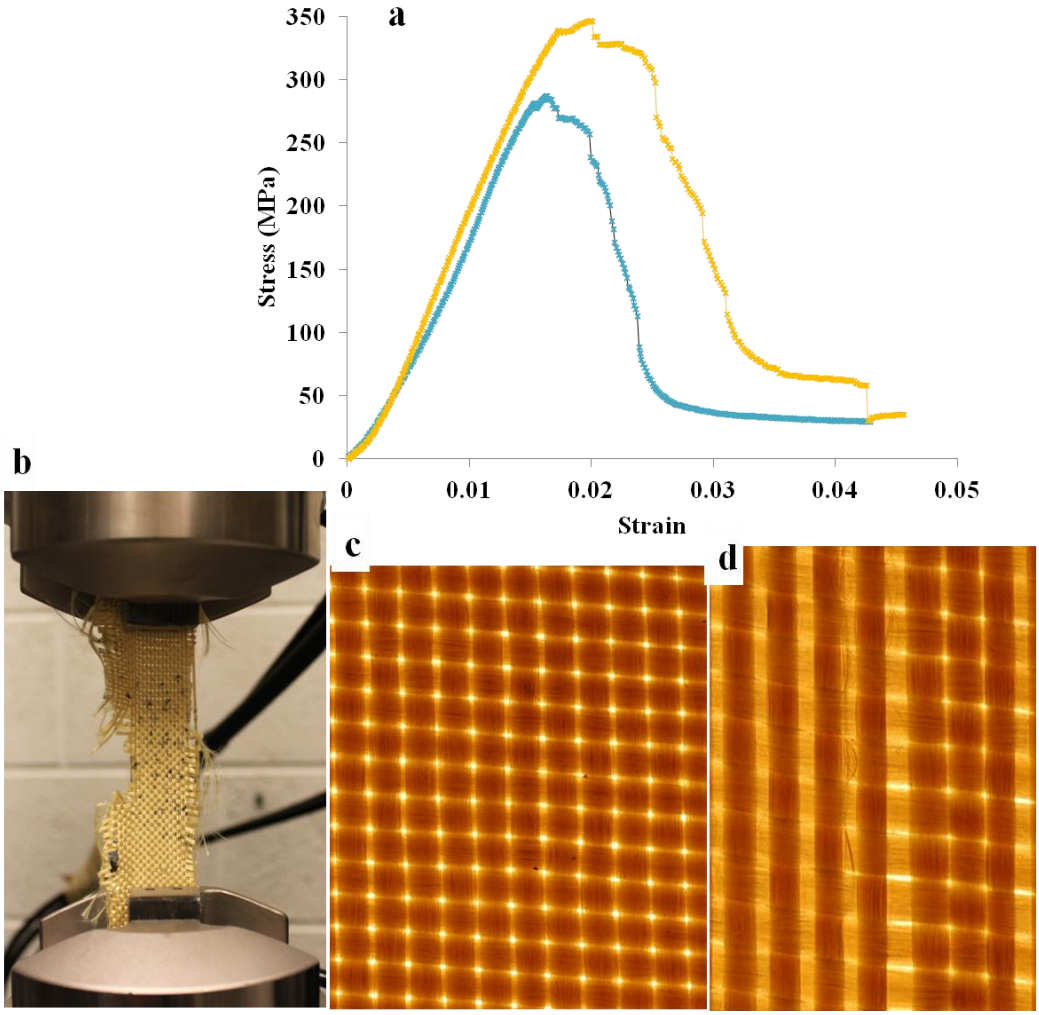

Figure S2. Uniaxial tensile testing of a commercial 0°/90° plain woven Kevlar mat at 0.005/s. a) Stress-strain curves of Kevlar mat. b) Kevlar mat was tested along the 0° fiber direction with fibers in the 90° direction free to slide. c) An image of the mat before testing and d) after testing with local failure by fiber breakage.

S3. The Effect of Potassium Cations

Potassium cations from the Kevlar/KOH/DMSO solution for ANFs formation do not remain attached to aramid backbones, thus they will not affect the network properties. During the dissolution of Kevlar microfibers in KOH/DMSO solution, the amide N-H bonds of aramid backbones were deprotonated.[17] As a result, negatively charged nitrogen ions were formed. The positive potassium ions in KOH stabilize the N anions on aramid nanofibers in the red Kevlar/KOH/DMSO solution. Once acid was added to the solution to induce hydrolysis, and given how basic the nitrogen anions are in nature, potassium cations re-protonated almost immediately. The pH of the solution during the hydrolysis stage was measured and dropped from initially basic to neutral (pH was 7), a pH level at which aramid would not be deprotonated, hence no potassium cations remained attached to aramid molecules. Furthermore, the water added during hydrolysis and GA polymerization or to make a “No Treatment” sample also immediately reprotonated aramids and washed potassium away from aramid backbone molecules.

S4. FTIR Spectroscopy of Liquid Products

The extent of the PA/GA treatment affected the chemical-structural changes in the networks. The differences of the chemical structures in the solid products (Figures 4 b.2 and b.3) and intermediate structures were not strongly discoverable via FTIR. Two distinct spectra, however, were observed for the liquid residues of the reactive processes after the solid parts had been filtered. The spectrum in **Figure S4.**a was consistently observed for reactive samples that had been prepared with a stoichiometric excess amount of PA and GA (Samples D and E, Figure 4.b.3). As a result, it is expected to represent a product solution with a large amount of terephthalic acid, formed due to extensive hydrolysis of the aramid backbone molecules. This prediction is supported by a broad peak (peak 1 in Figure S4.a, 3700-2500 cm^{-1}) which likely represents OH bonds and could arise from carboxylic acids and from water molecules that were formed during the condensation reaction. This result is consistent with the experimental condition of Samples D and E in which there were large amounts of excess GA and water in the liquid product. The set of peaks in the frequency range 1600-1400 cm^{-1} (peak 2 in Figure S4.a) represents different resonance forms of the highly conjugated C=O bonds present within the liquid, corresponding to the C=O from carboxylic acid and excess aldehydes [24].

The second characteristic spectrum (Figure S4.b) was observed for the liquid residue from reactions produced with less than the stoichiometric amounts of the PA/GA reagents (Sample A, Figure 4.b.2). The broad frequency range 3700-2500 cm^{-1} (peak 1 in Figure S4.a) associated with OH bond stretching from carboxylic acid and water was not present; instead, there was a broad signal between 3500 and 2500 cm^{-1} (peak 1 in Figure S4.b), that can be explained as arising overlaps of several groups: 1) C-H alkyl bonds between the carbons in dissolved GA could produce the signal at around 3000 cm^{-1}; 2) OH bonds from carboxylic acid produced after hydrolysis in the range between 3000-2500 cm^{-1}; and 3) C-H bonds from the aldehydes in GA at 3023 and 2933 cm^{-1}. The signals at frequencies between 2500 and

2000 cm^{-1} (peak 2 in Figure S4.b) likely correspond to phosphine and phosphorous groups formed from phosphoric acid in the reactive medium [24]. This peak (peak 2 in Figure S4.b) was more distinct when less than stoichiometric amounts were used owing to the decreased amounts of carboxylic acids present in Samples A to C compared to previous examples (Samples D and E) that had an excess of the reagents.

It is clear that there were important differences between the FTIR spectra of the two types of liquid residue. Those differences indicate that reducing the amount of PA/GA reagents led to a decreased extent of hydrolysis, with correspondingly fewer OH groups being formed and larger amounts of unreacted GA remaining (Figure S4.b). Figure S4.b with less than stoichiometric amounts of PA/GA regents showed a larger amount of saturated carbon groups with signals around 3000 cm^{-1} and a considerably smaller amount of OH groups as evidenced by the peak shift away from 3500 cm^{-1} (peak 1 in Figure S4.b). In addition, the signal around 2350 cm^{-1} (peak 2 in Figure S4.b) indicated that the phosphine groups in the second solution, produced with less than the stoichiometric quantities of the PA/GA reagents, were more prominent than in the first solution produced with excess reagents. This supports the claim that there were fewer OH groups present in the second solutions. Secondly, the C=O signal shifted to higher frequencies in the second solutions (peak 3 in Figure S4.b). This is an indication that the carboxylic groups were not as conjugated as those in the samples with excess reagents, so that the C=O groups probably came from GA rather than the aramid [24]. Those conclusions also support the proposed reaction mechanisms (Figure 3).

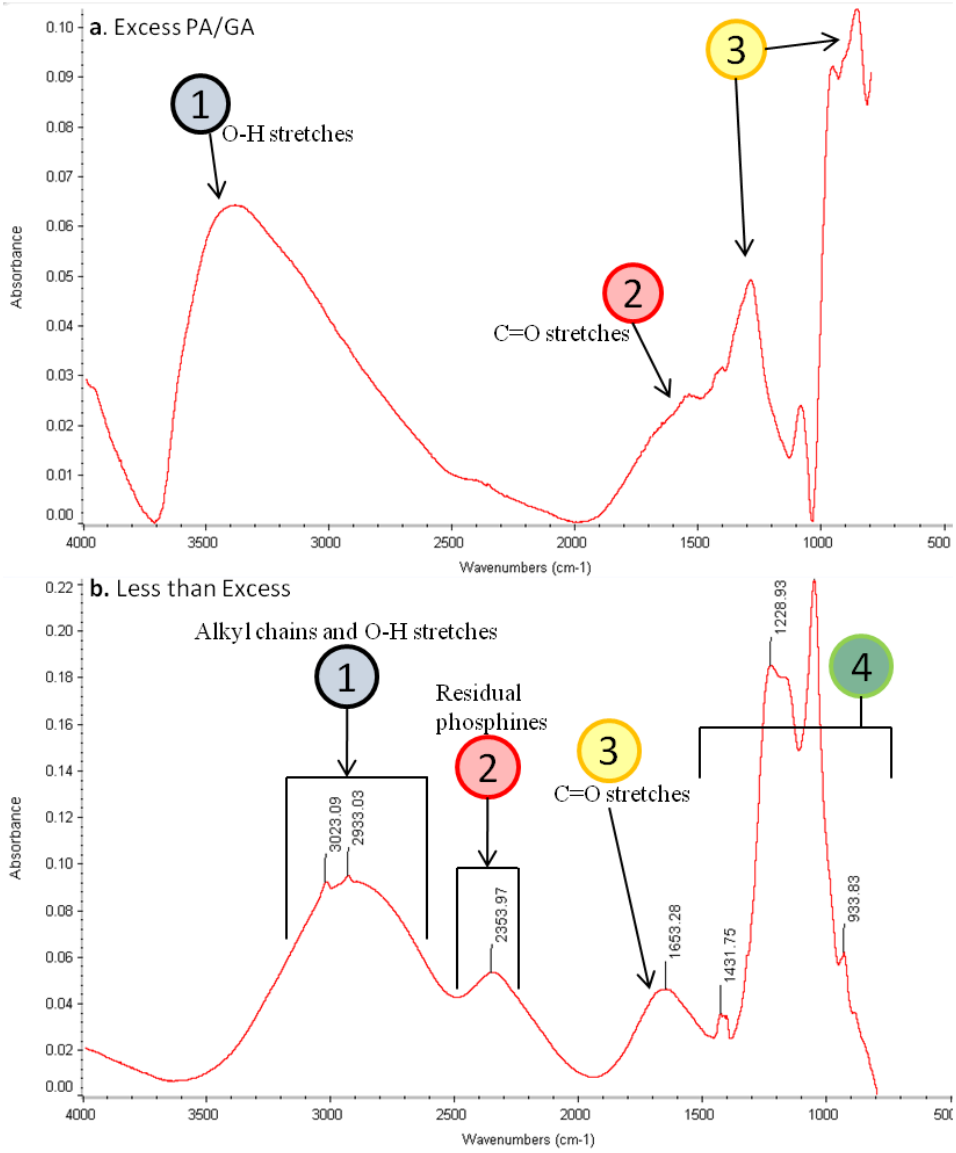

Figure S4. a) FTIR spectrum of the liquid product with extensive amounts of PA/GA reagents, showing peaks at 3350 cm^{-1}-(1), 1500 cm^{-1} (2), and the fingerprint region (3). b) FTIR spectrum of the liquid product with limited amounts of PA and GA, showing peaks at 3023 and 2993 cm^{-1}-(1), 2354 cm^{-1} (2), 1653 cm^{-1} (3), and the fingerprint region (4).

S5. DCE-Crosslinked ANF Network

A DCE-crosslinked ANF Network was made by slowly adding 10 mL of 1, 2-Dichloroethene (anhydrous, 99.8%, Sigma-Aldrich) into the Kevlar^{TM}/KOH/DMSO solution containing 100 mg Kevlar^{TM} while stirring over a period of two hours. The solid formed during this process was consolidated by the vacuum-assisted filtration method as discussed in section 4. DCE has a similar molecular structure to GA, but owing to its functional groups, DCE can react with aramid molecules without hydrolysis, the reaction mechanism and the TEM image of which are shown in **Figure S5** a and b. Figure S5.c shows that the stiffness and yield strength of the DCE-crosslinked ANF network were slightly higher than those of Sample A. The similarity of the stiffness and yield strength between the two samples indicates that the DCE sample had a similar structure (Figure S5.e) as Sample A (Figure 4.b.2), although the DCE sample had a higher ultimate strength and strain at failure probably owing to fewer defects introduced during synthesis without the hydrolysis step. FTIR spectrum of the DCE-crosslinked sample shown in Figure S5.d verified the reaction mechanism in Figure S5.a, which results in a structure shown in Figure S5.e. A DCE sample with 20 mL DCE (DCE-Kevlar+) was also made to insure that ANFs were crosslinked to the maximum amount, and this sample yielded identical mechanical properties as the sample with 10 mL DCE.

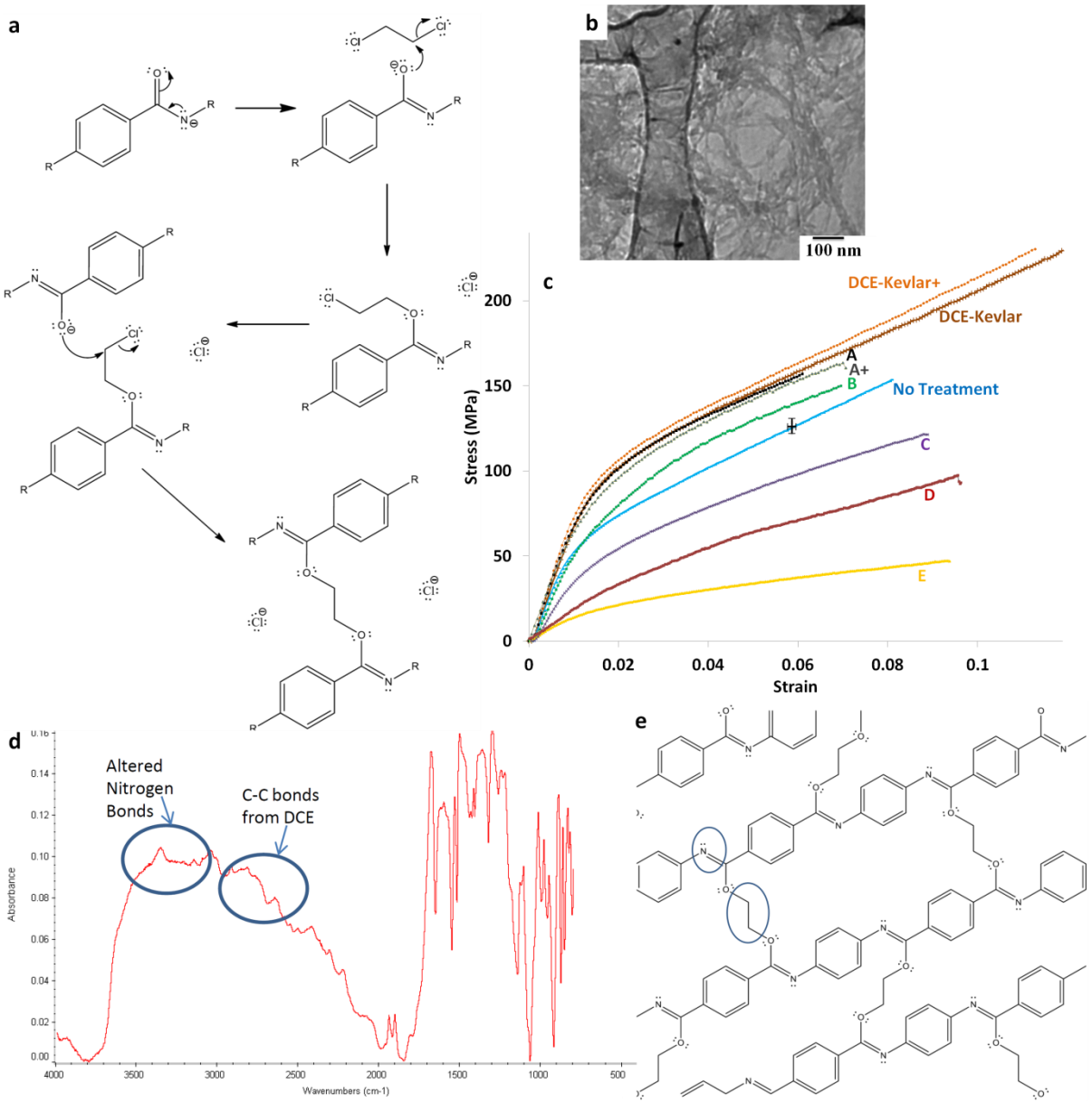

Figure S5. a) Reaction mechanism of DCE with aramid molecules. DCE crosslinks two aramid molecules with no hydrolysis. b) TEM image of the solid left after evaporation of the DCE-crosslinked ANF network dispersed in a DMSO solution. c) Stress strain curves of the PA/GA treated samples and the "No Treatment" sample from Figure 2.a compared with the DCE-crosslinked ANF networks, which have slightly higher stiffness and strength and greater ultimate strength and extensibility than those of Sample A. d) FTIR spectrum of the DCE-crosslinked networks and their corresponding structure (e).